Ultrasonics Sonochemistry 21 (2014) 1435–1440

Contents lists available at ScienceDirect

Ultrasonics Sonochemistry

journal homepage: www.elsevier.com/locate/ultson

Ultrasonic irradiation effects on electrochemical synthesis of ZnO nanostructures

Abazar Hajnorouzi [a], Reza Afzalzadeh [a,*], Faezeh Ghanati [b]

[a] Department of Solid State Physics, Faculty of Physics, K. N. Toosi University of Technology, POB 15875-4416, Tehran, Iran
[b] Department of Plant Biology, Faculty of Biological Science, Tarbiat Modares University, POB 14115-154, Tehran, Iran

ARTICLE INFO

Article history:
Received 16 November 2013
Received in revised form 29 December 2013
Accepted 8 January 2014
Available online 31 January 2014

Keywords:
ZnO nanoparticles
Electro-deposition
Ultrasonic irradiation
Ultrasonic bath calibration
ZnO nanosheets
Ultraviolet absorption

ABSTRACT

In the present article, electrochemical synthesis of ZnO nanostructures in presence of ultrasonic irradiation is investigated. The ultrasonic bath use for synthesis is calibrated using hydrophone method so that its frequency and acoustic power were obtained. From the results of the experimentation the role of ultrasonic irradiation in synthesis of ZnO nanoparticles is discussed. Diameter of the ZnO nanoparticles produced in the electrolyte was compared and investigated in absence and presence of the ultrasonic irradiation utilizing UV–visible photo-spectrometer. Then electrodeposited ZnO layer on the ITO glass as cathode's surface in absence and presence of the ultrasonic irradiation were studied by UV–visible photo-spectrometer and field emission scanning electron microscopy (FE-SEM) and the results were compared. FE-SEM micrographs show, higher growth of nanosheets on the cathode electrode in presence of ultrasonic irradiation. Experiment shows synthesis of ZnO nanoparticles in presence of the ultrasonic irradiation happen 10 times faster.

1. Introduction

Nano sized semiconductor particles have attracted great interests for technological applications because of their several interesting size dependent optical and electrical properties. Different properties of nanoparticles from those of bulk materials have encouraged many researchers to investigate these nano sized materials in various application fields [1–3].

Zinc oxide (ZnO) is a II–VI semiconductor with a wide and direct band gap of about 3.37 eV (at 300°K). It has a large exciton binding energy of 60 meV, high mechanical and thermal stabilities and radiation hardness [1]. It's interesting properties, such as transparency in the visible spectra and high infrared reflectivity, acoustic characteristics and direct band gap beside being cheap, abundant in nature, non-toxicity and easy for preparation have prompted its applications in a variety of industrial and technical fields [2] like; gas sensors, biosensors, biological labels, solar cells, electrochemical cells, varistors, ultraviolet (UV) photodiodes, electrical and optical devices and surface acoustic wave (SAW) devices [3]. Quantum confinement effects of ZnO nanostructures can enable continuous tuning of the emission and detection wavelengths to improved device performance [4].

Different methods for synthesis of ZnO nanostructures can be classified in three categories as follows; vapor phase such as PVD [5], solid phase such as combustion synthesis [6], and solution phase such as hydrothermal [7] and electrochemical [8,9].

Among the recent ZnO nanostructure synthesis techniques, ultrasonic irradiation have been widely employed in solution phase processes. Intensive sonication of a liquid generates bubbles by cavitations which then collapse causing a very high but momentary raise in temperature up to 5000 K and pressure up to 1800 atmospheres inside the collapsing cavity, known as the 'hot spot' [10], which is responsible for the homogeneous sonochemical reactions and deposition.

The proposed mechanism for the described reactions process is the following: When ultrasonic treatment is applied to aqueous solution of an inorganic salt, the ions of the salt are absorbed on or near the formed acoustic bubbles [11]. As the result of collapse these ions impact one another and nanoparticles of the inorganic salt are produced as a result of the influence of localized high temperatures and pressures. According to a report nucleation work needed for crystallization is strongly reduced by the presence of a liquid–gas bubble interface, therefore the presence of the bubble surface accelerates the crystal nucleation [12].This emission from the alkali metals arouse from the gas phase of the bubbles. Were collapse occurs, cavitation not only occurs in liquid, but also in liquid near a solid surface (glass slides) and it is found that the

* Corresponding author. Tel.: +98 2123064309; fax: +98 2123064218.
E-mail address: afzalzadeh@kntu.ac.ir (R. Afzalzadeh).

http://dx.doi.org/10.1016/j.ultsonch.2014.01.013
1350-4177/

presence of a solid surface increases the nucleation rate. Generated high-speed jets of the liquid, formed after the collapse of the bubble, throw the formed nanoparticles at high speed toward the glass slides [13].

Along with the advantages of solution phase growth methods, producing pure product using these methods is usually challenging due to the presence of surfactants which are usually added as size-controlling agents and by-products formed in the solution phase [8]. The electrochemical route as an alternative can offer the advantages of being simple and convenient with less difficulty, which facilitates the generation of pure, homogeneous and large quantities of particles [8].

In this research article, effects of using ultrasonic irradiation along with electrochemical techniques are investigated. The ZnO nanoparticles formed in the solution and nanosheets grown via electrochemical deposition in presence and absence of ultrasonic irradiation are discussed. The synthesized nanoparticles are analyzed using UV spectrometer and the morphology of ZnO nanosheets grown on ITO electrode were analyzed using FE-SEM.

2. Material and methods

The electrochemical synthesis was carried out in a two-electrode cell powered by a DC power supply 0–36V/0–3A (Arma, APS-1363P, Tehran, Iran). The clean Indium Tin oxide (ITO) coated glass sheets (active area of $1.0 \times 1.5\ cm^2$) with $50\ \Omega$ resistivity were used as working electrode (cathode), with another ITO as counter electrode (anode). ITO was rinsed ultrasonically for 15 min in acetone, isopropyl alcohol and ethanol, respectively. The zinc nitrate solution with 0.1 M was prepared using $Zn(NO_3)_2 \cdot 4H_2O$. Electrochemical synthesis of the zinc oxide (ZnO) nanoparticles in solution and the sheets on the ITO substrate were performed in a small beaker containing 4 ml of Zn^{+2} precursor liquid via constant potential of 0.85 V. In order to control the process temperature, the beaker was positioned in 20 °C water bath. The optical absorption of synthesized ZnO nanoparticles were measured every 1.5 min during the experimentation and after each measurement the solution was returned back in the beaker to continue the electrochemical synthesis for the next different times of exposure.

In the next step under the same electrochemical conditions, the beaker was positioned at a distance of 30 mm above the transducer axis in the bath to examine ultrasonic effects (see Secection 2.1). After fixing the bath water temperature on 20 °C, all devices such as thermometer, heater, etc. were removed from the bath to avoid ultrasonic mode changes and making the experiment repeatable. Just after each sonication, temperature of the bath is measured to increase only by 0.3 °C, in which before performing next sonication it returns backed to 20 °C. Ultrasonic agitation times for constant power were varied from 0 to 30 min, but only useful data are presented in this report.

The optical absorptions of the synthesized ZnO nanoparticles in the solution were measured with a Perkin–Elmer Lambda 25 UV–visible spectrometer in each 1.5 min intervals. A slit width of 1 nm and a sampling interval of 0.5 nm were used to record the spectra between 250 to 500 nm. The solution of 0.1 M zinc nitrate was used as the blank solution (reference). The ITO cathode sample was characterized by UV–visible spectrometer in absorption mode and the surface morphology is studied by using field emission scanning electron microscopy (FE-SEM, Philips-4160).

2.1. Calibration of the ultrasonic bath

Calibration of acoustic pressure of the bath was carried out using hydrophone method in the cubic chamber with calibration range from 10 kHz to 20 MHz, with a sensor diameter of 25 mm. The bath (digital Ultrasonic cleaner- CD-4820, China) with the dimensions of $80 \times 150 \times 250\ mm^3$ was filled with 2500 ml water. A hydrophone PVDF-type (PA124, Precision Acoustics Ltd, Dorchester, Dorset, UK) was located at a distance of 30 mm from the bottom of a 100 ml beaker which was full of water. In order to record, measure and process the ultrasonic signals the hydrophone was connected to a digital oscilloscope (TNM 20080, TNM Electronics Ltd., Tehran, Iran) and then to the computer [14,15]. The real frequency and acoustic pressure (P_A) of the ultrasonic bath measured were 36.62 kHz and 19.6 atmospheres respectively, for fundamental frequency based on calibration certification test results.

Fast Fourier transform (FFT) analysis is used to obtain, the frequency content of a captured signal. In order to extract the frequency contents of driven data, signals were analyzed in MATLAB software version 7.0.1 (Math Software Co., Math works, USA) using FFT function. Calibration data for piston hydrophone at 36.62 kHz frequency is 1.681 μV/Pa, which the acoustic pressure is equal to 19.62 atmospheres. The measured signal amplitude versus frequency for the bath is shown in Fig. 1.

3. Results and discussion

The results of the experimentation are presented and discussed in three sections to investigate the effect of ultrasonic irradiation on size of the synthesize ZnO nanoparticles and effects on electrochemical deposition of ZnO on ITO substrate.

3.1. Effect of ultrasonic irradiation on particle size

The absorption spectra were taken from the zinc nitrate solution containing electrochemically synthesized ZnO at different time intervals comparatively, in the absence and presence of the ultrasonic irradiation. The UV absorption spectrum with well-defined exciton peaks of ZnO are observed in measurements for different cases and presented in Fig. 2. UV absorption edge in absence of ultrasonic shown in Fig. 2a have no significant peak shift but in Fig. 2b upto 13.5 min have blue shift but after passing 13.5 min no significant shift is observed. Magnitude of absorption in absence of ultrasonic is 0.08 while in presence of ultrasonic is 0.85 for equal synthesis time of 19.5 min as a typical case. Magnitude of absorption indicates amount of the ZnO produced, which shows in the presence of the ultrasonic irradiation, production of the ZnO nanoparticles is increased by 10 times.

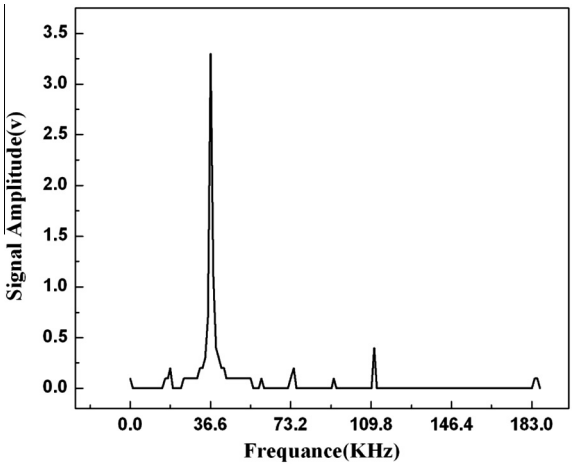

Fig. 1. Signal amplitude vs. frequency for ultrasonic bath obtained by FFT.

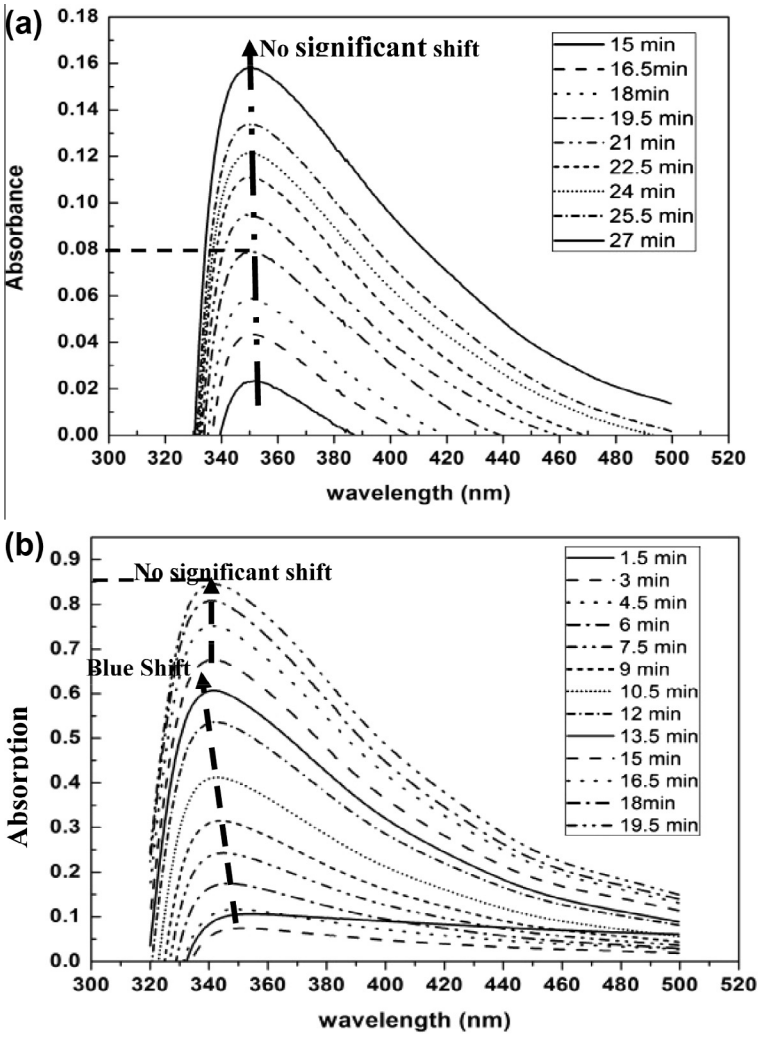

Fig. 2. UV–visible Spectrums of the ZnO colloids produced in 20 °C, for different times in**; (a)** absence and **(b)** presence of the ultrasonic irradiation.

Experiments are carried in absence of ultrasonic for 27 min, while in presence of ultrasonic only up to 19.5 min because absorption peak have reached to near the maximum absorption.

Fig. 3 shows UV-absorption diagram in absorption mode for ZnO deposited electrochemically on the ITO glass under ultrasonic irradiation, while using another clean ITO glass as the reference.

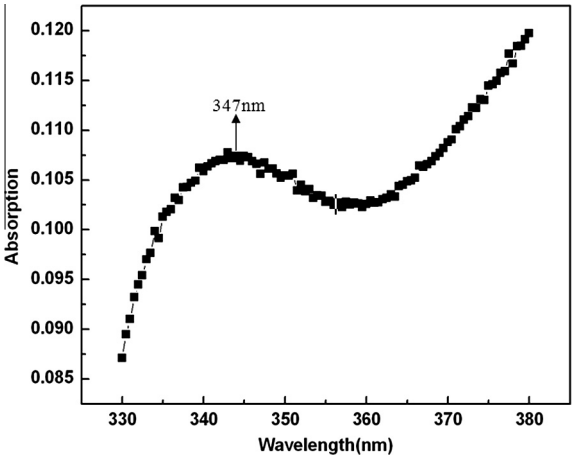

Fig. 3. UV-absorption spectrum of ZnO deposited on the ITO substrate in the presence of the Ultrasonic irradiation.

UV absorption edge, indicated in Fig. 3 is 347 nm, which shows the size of the synthesized ZnO is in the quantum regime. UV absorption for the ITO cathode surface in absence of the ultrasonic irradiation has no significant peak (data are not shown). It may be due to deposition of thinner layer on the cathode surface in absence of the ultrasonic irradiation compared to the presence of the ultrasonic irradiation.

The electro-synthesis of ZnO is obtained due to a series of reactions occurring at two electrodes as well as in the electrolyte. Passing electrical current under applied potential of 0.85 V, which is accordance to Nurnst equation [16]. The following reactions occur:

$$2H_2O \rightarrow O_2 + 4H^+ + 4e^- \quad (1)$$

$$2NO_3^- + H_2O + 2e^- \rightarrow N_2O_5 + 2OH^- \quad (2)$$

$$Zn^{+2} + 2\,OH^- \rightarrow Zn(OH)_2 \downarrow \quad (3)$$

$$Zn(OH)_2 + 2OH^- \rightarrow Zn(OH)_4^{-2} \quad (4)$$

$$Zn(OH)_4^{-2} \rightarrow ZnO \downarrow + H_2O + 2OH^- \quad (5)$$

Water oxidation occurs (reaction 1) at the anode, while NO_3^- ions in the solution undergo reduction (reaction 2) at the surface of cathode to produce OH^- ions [17]. Electro-generation of hydroxide (OH^-) results in Zn $(OH)_2$ production (reaction 3).

The concentration of OH^- ions increases as time passes and correspondingly $Zn(OH)_2$ and/or ZnO nuclei are formed in solution according to reactions 4 and 5 [8]. Reaction 1 occurs at anode, reaction 2 at cathode, and reactions 3 to 5 occur both in the solution and at the cathode surface.

The average particle size formed in colloid is calculated from the absorption onset using the effective mass model [18,19] and use of the following equation [20]:

$$r(\mathrm{nm}) = \frac{-0.3049 + \sqrt{-26.23012 + 10240.72/\lambda_p(\mathrm{nm})}}{-6.3829 + 2483.2/\lambda_p(\mathrm{nm})}. \quad (6)$$

Electrolysis reaction time is varied from 0 to 30 min. The UV-absorption of the electrolyte solution was taken each 1.5 min intervals and then corresponding wavelength of UV-absorption peaks were used to calculate particles diameters from Eq. (6) for different times of synthesis in presence and absence of ultrasonic irradiation. The data are extracted from ultraviolet absorption peaks (UV absorption edge) from Fig. 2. These data are presented in Table.1 for easier comparison of the particles sizes.

UV absorption edge in Table.1 shows wavelengths from 355.59 to 341 nm which indicates significant blue-shifted compared to the absorption onset of bulk zinc oxide which is 385 nm. This information indicates that the average particle size is in the quantum size range [18].

For the experiments done without ultrasonic irradiation, the first absorption peak is appeared after 15 min while under ultrasonic irradiation the first absorption peak is observed after only 1.5 min that is 10 times faster. Such reduction in production time of ZnO nanoparticle is very important for large scale production point of view.

Fig. 4 shows diameter-time diagram of ZnO nanoparticles produced in absence and presence of ultrasonic irradiations during electrochemical synthesize.

In the absence of ultrasonic irradiation, ZnO nanoparticles get formed slowly so the decrease in number of ions in the solution is very slow and as a result, the diameter of nanoparticles synthesized at different times tested is approximately constant versus time. While in presence of ultrasonic irradiation after 1.5 min, nanoparticles with diameter of 4.32 nm are synthesized. As time passes, the diameter of nanoparticles decrease, therefore the UV-absorption diagram show a blue shift until it reaches to the final diameter of 3.66 nm. In the presence of ultrasonic irradiation, the ZnO nanoparticles rapidly get formed in the electrolyte solution and on passing time, reduction in size and further saturation in the curve as shown in Fig. 4 is observed. Curve fitting for the diameter-time diagram gives R^2 value to be 0.99 that is indicating good fitting and leads to a exponential equation,

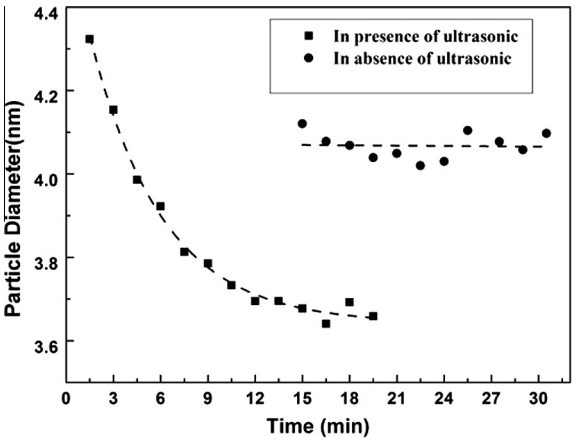

Fig. 4. Diameter of nanoparticle synthesized versus time in presence and in absence of ultrasonic irradiation (dash line is fitting curve).

$$D(\mathrm{nm}) = 3.64 + 0.95e^{(-t/4.59)}. \quad (7)$$

In presence of ultrasonic irradiation, Eq. (7) can be expected to be non-linear due to drastic change in precursor concentration during the experimentations. Initially large amount of precursor is present therefore diameter of produced ZnO nanoparticle grown is largest. Because of using only 4 ml precursor in a small beaker, it decreases rapidly therefore resulting in formation of smaller nanoparticles, later. We have used small beaker because in electrodeposition, anode and cathode should be close to each other to have less convection and therefore more solution uniformity.

We know ZnO nanoparticles move randomly in solution due to wave pressure and also Brownian motion. When a bubble is present in the path of a particle (here is ZnO), either it enters the bubble (bubble collapse) or it sits on the surface of the bubble depending on kinetic energy of particle, size of bubble and surface tension of liquid. Due to collision of the larger particles (4.3 nm) formed initially with surface of the substrate and sticking, causes reduction in precursor, therefore diameter of the further produced nanoparticles in electrolyte is expected to be smaller (see Section 3.3).

3.2. Role of the ultrasonic irradiation in the synthesis of the ZnO nanoparticles

For the said precursor Zn^{+2}, OH^- and $Zn(OH)_4^{-2}$ ions are produced via electrolysis synthesis (Eqs. (1) to (4)). This ions move randomly with high speeds due to Brownian motion and wave pressure. When these ions reach to the bubble surface, stop and sit on the outer surface of the bubbles, which for larger bubble,

Table 1
UV absorption edges and calculated diameters of the ZnO nanoparticles for different time with and without ultrasonic irradiation.

Time (min)	Electrochemical synthesis			
	Without ultrasonic irradiation		With ultrasonic irradiation	
	UV absorption edge (nm)	Diameter (nm)	UV absorption edge (nm)	Diameter (nm)
1.5	Not formed	Not applicable	355.59	4.32
3.0	"	"	352.47	4.15
4.5	"	"	348.99	3.98
6.0	"	"	347.58	3.92
7.5	"	"	345.00	3.81
9.0	"	"	344.31	3.78
10.5	"	"	342.98	3.73
12.0	"	"	341.98	3.69
13.5	"	"	342.00	3.69
15.0	351.80	4.12	341.51	3.68
16.5	350.94	4.08	340.51	3.64
18.0	350.75	4.08	341.91	3.69
19.5	350.14	4.04	341.00	3.66

more ions get accommodated on the surface. Maximum radius R_{Max} and collapse time τ of bubble can be calculated by Eq. (8) [21];

$$R_{Max} = \sqrt{\frac{3\gamma P_A}{4\pi^2 \nu^2 \rho}} \quad \tau = R_{Max}\sqrt{\frac{\rho}{p_A + p_h}}. \tag{8}$$

Where ν is the applied acoustic frequency which is 36.62 kHz, P_A is acoustic pressure measured to be 19.6 atmospheres, and P_h the external pressure is around 1 atmosphere.

Maximum radius of the bubble is calculated by Eq. (8), to be 0.395 mm in the present conditions, therefore surface of the bubble is 1.95 mm^2 while ionic radius is in order of Pico meter, therefore large amount of ions can sit on the bubble surface. Collapse time is calculated from Eq. (8) to be about 8 μs. This collapse time is very short; therefore speed of ions collision due to micro jet effects is high enough to promote the reaction of formation of ZnO nanoparticles.

The maximum temperature and pressure inside a collapsing transient bubble can be calculated by assuming adiabatic bubble collapse [22,23].

$$T_{Max} = \frac{T_0 P_A(\gamma - 1)}{P_v} \quad P_{Max} = P_v \left(\frac{P_A(\gamma - 1)}{P_v}\right)^{\left(\frac{\gamma}{\gamma - 1}\right)} \tag{9}$$

Where T_0 is the liquid temperature, P_A is the acoustic pressure at initiation of collapse, γ is the ratio of specific heats of dissolved gas or vapor, P_v is the vapor pressure of solvent. Calculated collapse pressure is 1.6×10^7 atmosphere and T_{max} is 148,800 K from Eq. (9).

As a result, absorbed ions on the bubble which are exposed to these extreme localized conditions start to impact one another and ZnO nanoparticles are produced [11,19]. This procedure is given in Eq. (10) and Eq. (11), also schematically shown in Fig. 5.

$$Zn^{2+} + 4OH^- \rightarrow Zn(OH)_4^{-2} \tag{10}$$

$$2(Zn(OH)_4^{-2}) \rightarrow 2ZnO + 4H_2 + 3O_2. \tag{11}$$

3.3. Role of ultrasonic irradiation on Electrochemical deposition of ZnO

ZnO nanosheets were formed by reduction of nitrate anion and production of hydroxide anion according to Eqs (3)–(5). Fig. 6 and Fig. 7 show FE-SEM micrographs of the cathode, giving morphology of electro-deposited ZnO on the ITO surface in absence and presence of the ultrasonic irradiation respectively. Dashed squared in Figs. 6a and 7a are shown in Figs. 6b and 7b with bigger scale respectively. Applying ultrasonic irradiation during electrochemical deposition resulting in vertical growth of nanosheets on the ITO cathode shown in Fig. 7, which is further and greater growth of ZnO material observed in Fig. 6.

The size of nanosheets grown under ultrasonic irradiation synthesis (Fig. 7) is in order of few micrometers. As previously outlined (Fig. 5), the reason may be due to the effect of bubbles absorbed on solid surfaces such as cathode surface. Imagine a bubble sticks to surface of the substrate and many ZnO nanoparticles have sited on the bubble, when collapse occurs the nanoparticle collides with the substrate with high energy due to micro jet effect. Collision of the ZnO nanoparticles with the substrate can be in three forms i.e. inelastic, elastic or semi-elastic. Elastic collision cannot deduce growth of ZnO on the ITO glass because nanoparticles collide and bounce back to the electrolyte. But for inelastic collisions, when nanoparticles collide, stick to the substrate and therefore the initially formed larger particles (4.3 nm) get eliminated from the solution and as time passes reduction of precursor occurs. As possibility of collision with higher grown edges of the

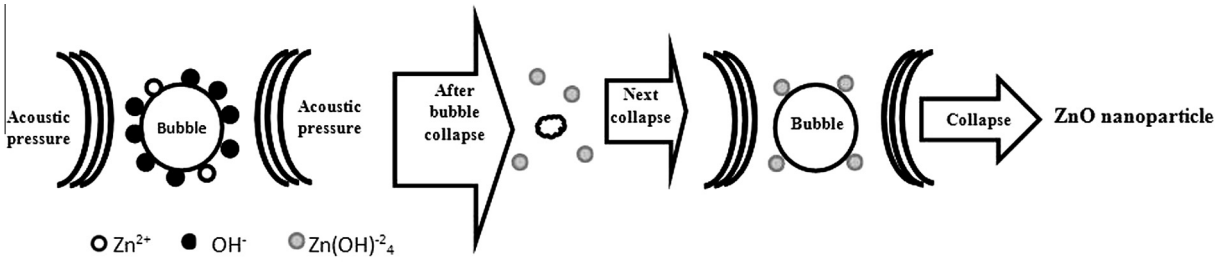

Fig. 5. schematic representation of the synthesis of ZnO nanoparticles under ultrasonic irradiation.

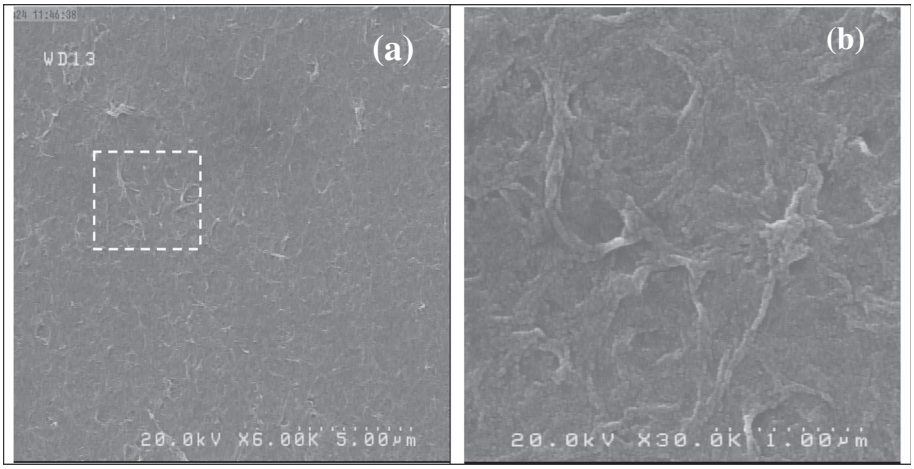

Fig. 6. FE-SEM micrograph of the ITO cathode surface under electrochemical-deposition.

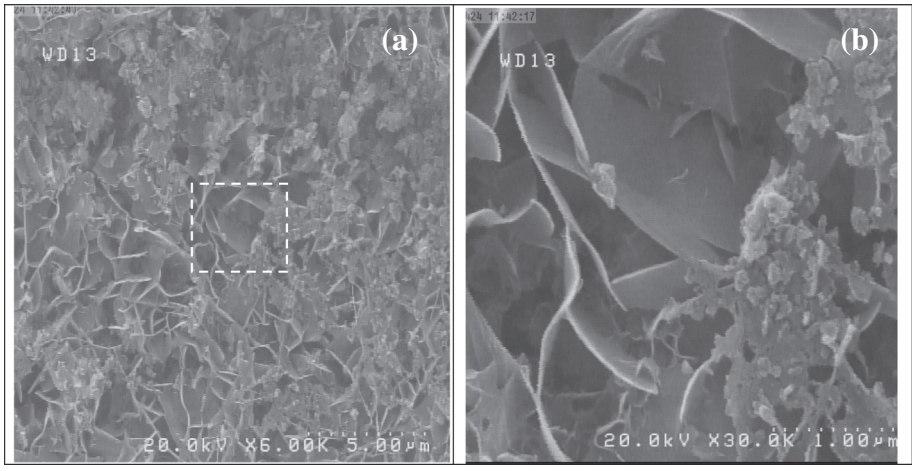

Fig. 7. FE-SEM micrograph of the ITO cathode surface under electrochemical deposition in presence of the Ultrasonic irradiation.

sheets in vertical direction is more, so it attaches to higher grown part of nanosheets causing much more growth of the nanosheets.

4. Conclusion

Applied ultrasonic irradiations along with electrochemical synthesis of ZnO nanoparticles make the production of the ZnO nanoparticles much faster and more efficient. The time needed for formation of the ZnO nanoparticles from the zinc nitrate electrolyte with electrochemical synthesis, has decreased by factor of 10 when ultrasonic irradiation is applied compared to the case without ultrasonic. In the presence of ultrasonic irradiations, earlier formed ZnO nanoparticles are larger in size (only 4.32 nm). Immediate deposition of these larger ZnO nanoparticles as nanosheets on cathode surface leads to elimination of these electrolyte and as a result decrease in diameter of the next generated ZnO nanoparticles' was observed. When deposition on cathode surface is followed only by electrochemical deposition, a very thin layer of ZnO gets coated on the cathode, while in presence of the ultrasonic irradiation, collapse of bubbles lead to higher formation rate of ZnO in the solution or deposition on the cathode's surface. Synthesis with use of ultrasonic irradiations can be easily controlled and it is expected to be applicable for production of nanoparticles with specific required diameters and faster rate for thicker deposition on cathode.

Acknowledgement

Authors would like to thanks Dr. Manijhe Mokhtari-Dizaji, for her support of using ultrasonic calibration instruments and useful discussions. Also authors would like to thanks Miss ashraf Heydaripour for her suggestions and useful discussions on electrochemical methods.

References

[1] D. Polsongkram, P. Chamninok, S. Pukird, L. Chowb, O. Lupan, G. Chai, H. Khallaf, S. Park, A. Schulte, Effect of synthesis conditions on the growth of ZnO nanorods via hydrothermal method, Physica B 403 (2008) 3713–3717.
[2] Haining Chen, Weiping Li, Qin Hou, Huicong Liu, Liqun Zhu, A general deposition method for ZnO porous films: occlusion electrosynthesis, Electrochim. Acta 56 (2011) 9459–9466.
[3] Davood Raoufi, Synthesis and microstructural properties of ZnO nanoparticles prepared by precipitation method, Renew. Energy 50 (2013) 932e937.
[4] Liqiao Qin, Christopher Shing, Shayla Sawyer, Partha S. Dutta, Enhanced ultraviolet sensitivity of zinc oxide nanoparticle photoconductors by surface passivation, Opt. Mater. 33 (2011) 359–362.
[5] Lisheng Wang, Xiaozhong Zhang, Songqing Zhao, Guoyuan Zhou, Yueliang Zhou, Junjie Qi, Synthesis of well-aligned ZnO nanowires by simple physical vapor deposition on *c*-oriented ZnO thin films without catalysts or additives, Appl. Phys. Lett. 86 (2005) 024108.
[6] A. Jagannatha Reddy, M.K. Kokila, H. Nagabhushana, J.L. Rao, C. Shivakumara, B.M. Nagabhushana, R.P.S. Chakradhar, Combustion synthesis, characterization and Raman studies of ZnO nanopowders, Spectrochim. Acta Part A, 81 (2011) 53–58.
[7] Narges Kiomarsipour, Reza Shoja Razavi, Hydrothermal synthesis and optical property of scale- and spindle-like ZnO, Ceram. Int. 39 (2013) 813–818.
[8] T.G. Venkatesha, Y. Arthoba Nayaka, R. Viswanatha, C.C. Vidyasagar, B.K. Chethana, Electrochemical synthesis and photocatalytic behavior of flower shaped ZnO microstructures, Powder Technol. 225 (2012) 232–238.
[9] Y. Leprince-Wang, G.Y. Wang, X.Z. Zhang, D.P. Yu, Study on the microstructure and growth mechanism of electrochemical deposited ZnO nanowires, J. Cryst. Growth 287 (2006) 89–93.
[10] Prantik Banerjee, Sampa Chakrabarti, Saikat Maitra, Binay K. Dutta, Zinc oxide nano-particles – sonochemical synthesis, characterization and application for photo-remediation of heavy metal, Ultrason. Sonochem. 19 (2012) 85–93.
[11] Stella Kiel, Olga Grinberg, Nina Perkas, Jerome Charmet, Herbert Kepner, Aharon Gedanken, Forming nanoparticles of water-soluble ionic molecules and embedding them into polymer and glass substrates, Beilstein J. Nanotechnol. 3 (2012) 267–276.
[12] Anna Kordylla, Thomas Krawczyk, Feelly Tumakaka, Gerhard Schembecker, Modeling ultrasound induced nucleation during cooling crystallization, Chem. Eng. Sci. 64 (2009) 1635–1642, http://dx.doi.org/10.1016/j.ces.2008.12.030.
[13] Mersmann, A. Crystallization Technology Handbook, second ed., Marcel Dekker, Inc, 2001, pp. 58–67 (doi:10.1201/9780203908280).
[14] H. Hasanzadeh, M. Mokhtari-Dizaji, S.Z. Bathaie, Z.M. Hassan, V. Nilchiani, H. Goudarzi, Enhancement and control of acoustic cavitation yield by low level dual frequency sonication: a subharmonic analysis, Ultrason. Sonochem. 18 (2011) 394–400.
[15] H. Hasanzadeh, M. Mokhtari-Dizaji, S.Z. Bathaie, Z.M. Hassan, Evaluation of correlation between chemical dosimetry and subharmonic spectrum analysis to examine the acoustic cavitation, Ultrason. Sonochem. 17 (2010) 863–869.
[16] Allen. J Bard, L.R Faulkner, Electrochemical methods: Fundamentals and applications, second Ed, John-Wiley & sons, New York, 2001.
[17] J. Lee, Y. Tak, Electro deposition of ZnO on ITO electrode by potential modulation method, Electrochem. Solid-State Lett. 4a (2001) 63–65.
[18] Hu Zeshan, Gerko Oskam, Peter C. Searson, Influence of solvent on the growth of ZnO nanoparticles, J. Colloid Interface Sci. 263 (2003) 454–460.
[19] Raghvendra S. Yadav, Priya Mishra, Avinash C. Pandey, Growth mechanism and optical property of ZnO nanoparticles synthesized by sonochemical method, Ultrason. Sonochem. 15 (2008) 863–868.
[20] Satyanaray ana Talam, Srinivasa Rao Karumuri, Nagarjuna Gunnam, Synthesis, Characterization, and Spectroscopic Properties of ZnO Nanoparticles, International Scholarly Research Network ISRN Nanotechnology, vol. 2012 (doi:10.5402/2012/372505).
[21] M.H. Entezari, P. Kruus, Effect of ferquancy on sonochemical reactions, oxidation of iodide, Ultrason. Sonochem. 1 (1994) S75–S79.
[22] D. Drijvers, H.V. Langenhove, K. Vervaet, Sonolysis of chlorobenzene in aqueous solution: organic intermediates, Ultrason. Sonochem. 5 (1998) 13.
[23] E.A. Neppiras, Acoustic Cavitation, Phys. Rep.-Rev. Sec. Phys. Lett. 61 (1980) 159–251.